A remarkable effect of *N*,*N*-diethylamino functionality on the optoelectronic properties of a salicylimine-based probe for Al^{3+}

Neeraj, ‡[1]Ajit Kumar,‡[1] Virendra Kumar,[1] Rahul Prajapati,[1] Sharad Kumar Asthana,[1] K. K. Upadhyay,[1*] Jianzhang Zhao[2]
[1]*Department of Chemistry (Centre of Advanced Study), Faculty of Science, Banaras Hindu University, Varanasi, Uttar Pradesh-221005, India*
[2]*State Key Laboratory of Fine Chemicals, Dalian University of Technology, Dalian 116012, China*

***E-mail:** drkaushalbhu@yahoo.co.in; kku@bhu.ac.in; **Tel:** +91 542-6702488
‡These authors contributed equally to this work.

---

1. EXPERIMENTAL

1.1 Apparatus:

The IR Spectra for the **SA1** was recorded on JASCO-FTIR Spectrophotometer while ^{1}H NMR and ^{13}C NMR spectra for the same were recorded on a JEOL AL 300 FT NMR Spectrometer. Mass spectrometric analysis was carried out on a MDS Sciex API 2000 LCMS spectrometer. Electronic spectra were recorded at room temperature (298 K) on a UV-1700 pharmaspec spectrophotometer with quartz cuvette (path length=1 cm). Emission spectra were recorded on JY HORIBA Fluorescence spectrophotometer.

1.2 Materials:

All reagents for synthesis were purchased from Sigma-Aldrich and were used without further purification.

1.3 General Methods:

All titration experiments were carried at room temperature. All the cations were used as their chloride/nitrate salts while anions were used as their tetrabutyl ammonium (TBA) salts. The ^{1}H NMR spectra were recorded by using tetramethylsilane (TMS) as an internal reference standard. For the ^{1}H NMR spectra of **SA1**, 5×10^{-3} M solutions was prepared in DMSO-d_6 while the stock solution of Al^{3+} was prepared in DMSO-d_6:D_2O (95:5, v/v).

For UV-visible/fluorescence titration experiments, the solutions of cations were prepared in aqueous medium. Chloride/nitrate salts of metal were used for solution preparation. Due to insufficient solubility of **SA1** in pure water its stock solution of 0.25 M was prepared in ethanol which was used for fluorescence titration experiment in water at 0.1 μM concentration through dilution.

The detection limit of **SA1** towards Al^{3+} was determined from a plot of fluorescence intensity as a function of the concentration of the added Al^{3+}. To determine the S/N ratio, the fluorescence intensity of **SA1** in absence of any analyte was measured by 10 times and the standard deviation of blank measurements was determined. The detection was calculated as three times the standard deviation from the blank measurement (in the absence of analyte) divided by the slope of calibration plot between analyte concentration and fluorescence intensity.

X-ray crystallographic studies:

Single crystal X-ray diffraction measurements were carried out on an Oxford Diffraction Xcalibur system with a Ruby CCD detector. All the determinations of unit cell and intensity data were performed with graphite-mono-chromated Mo-K*α* radiation (λ= 0.71073 A°). Data for the ligand and metal complex were collected at room temperature. The structures were solved by direct methods, using Fourier techniques, and refined by full-matrix least-squares on F2 using the SHELXTL-97 program package [1]. Crystal data and details of the structure determination for ligand and complex are summarized in Table 1. CCDC **943713, 959758** and **959759** contains the supplementary crystallographic data for this paper. These data can be obtained free of charge from the Cambridge Crystallographic Data Centre via http://www.ccdc.cam.ac.uk/cgi-bin/catreq.cgi.

References:

1. (a) G. M. Sheldrick, SHELXL-97, Program for X-ray Crystal Structure Refinement, Göttingen University, Göttingen, Germany, 1997; (b) G. M. Sheldrick, SHELXS-97, Program for X-ray Crystal Structure Solution, Göttingen University, Göttingen, Germany, 1997.

Figure and Captions

Figure S1: ^{1}H NMR spectrum of **SA1** (in DMSO–d_6):

Figure S2: ^{13}C NMR spectrum of **SA1** (in DMSO–d_6):

Figure S3: IR spectrum of **SA1**:

Figure S4: Mass spectrum of **SA1**:

Figure S5: ^{1}H NMR spectrum of **SA1**+Al^{3+} Complex (in DMSO–d_6):

Figure S6: ^{13}C NMR spectrum of **SA1**+Al^{3+} Complex (in DMSO–d_6):

Figure S7: IR spectrum of **SA1**+Al^{3+} Complex:

Figure S8: Mass spectrum of **SA1**+Al^{3+} Complex:

Figure S9: UV–visible spectra of **SA1** with different metal ions at 10 μM in aqueous medium:

Figure S10: UV-visible titration spectrum of in 10 μM aqueous solution of **SA1** with **(a)** Fe^{3+} and **(b)** Cu^{2+} :

Figure S11: Visible color responses of **SA1** in the presence of various metal ions:

Figure S12: Emission spectra of **SA1** in the presence of $AlCl_3$ and $Al(NO_3)_2$:

Figure S13: Job's plot of **SA1** with Al^{3+} showing 2:1 binding stoichiometry:

Figure S14: Non-linear fit plot of fluorescence titration data for determination of binding constants:

Figure S15: ^{1}H NMR titration studies of **SA1** with Al^{3+}:

Figure S16: Fluorescence spectral changes of **SA1** and its Al^{3+} complex in the presence of H^+ ion:

Figure S17: Calibration curve for determination of detection limit of **SA1** for Al^{3+}:

Figure S18: Fluorescence changes at 471 nm of **SA1** (0.5 μM) and **SA1** + Al^{3+} (10 equiv.) in aqueous solution at different pH scale.

Table 1: Crystal Data and Details of the Structure Determination for **SA1** and its complexes with Cl^-/NO_3^-

Figure S1: ^{1}H NMR spectrum of **SA1** (in DMSO–d$_6$):

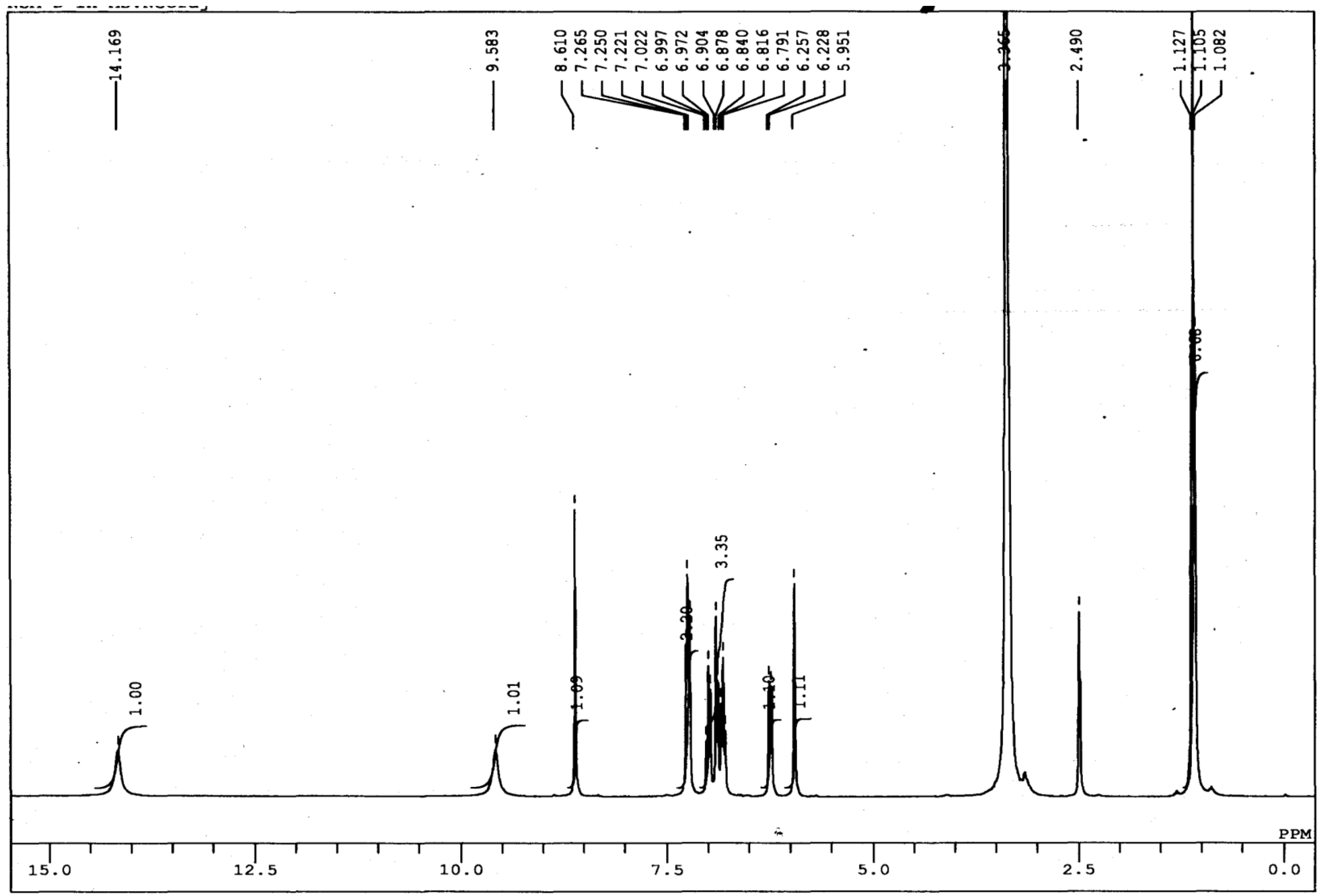

Figure S2: ^{13}C NMR spectrum of **SA1** (in DMSO–d_6):

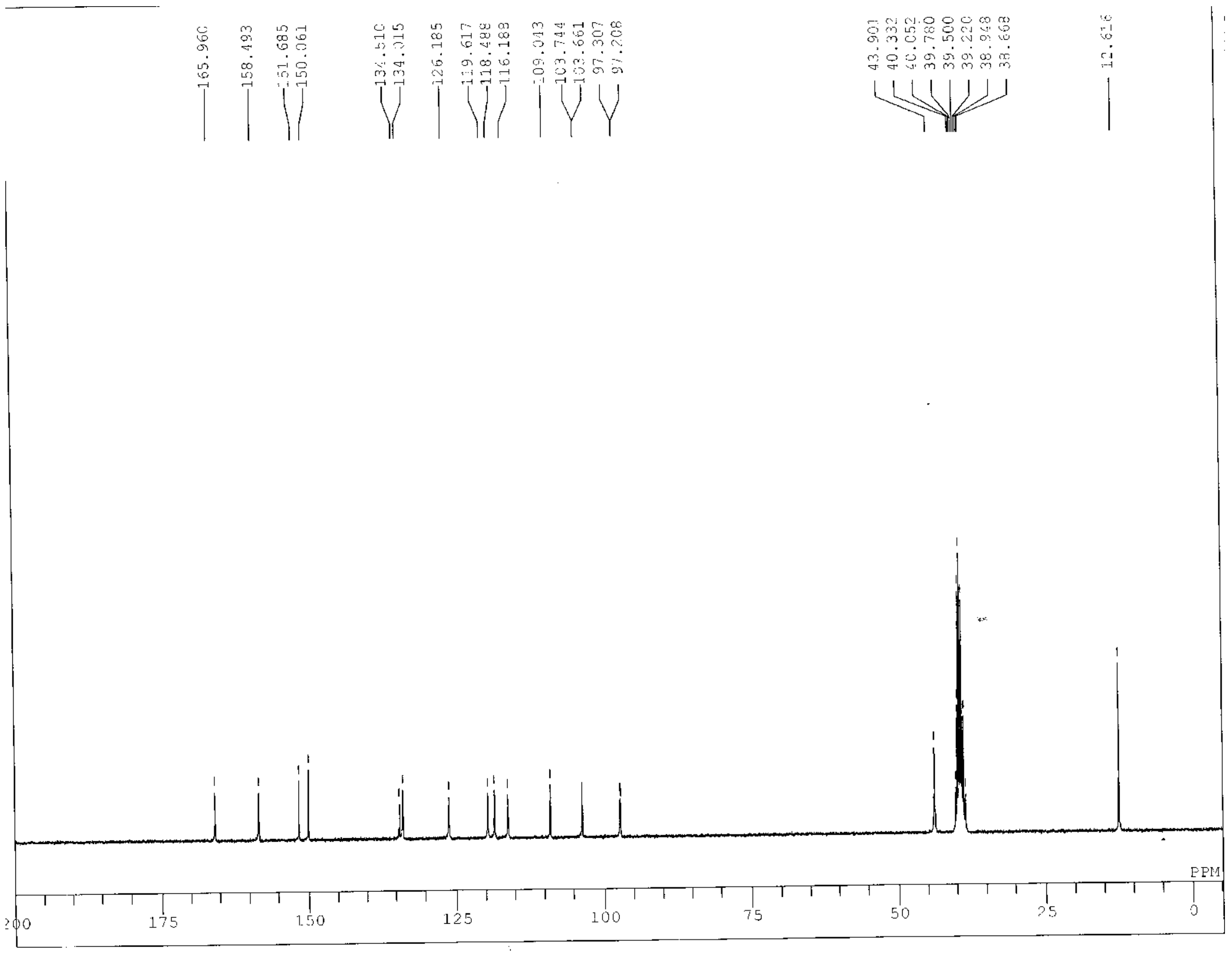

Electronic Supplementary Material (ESI) for Dalton Transactions

Figure S3: IR spectrum of **SA1**:

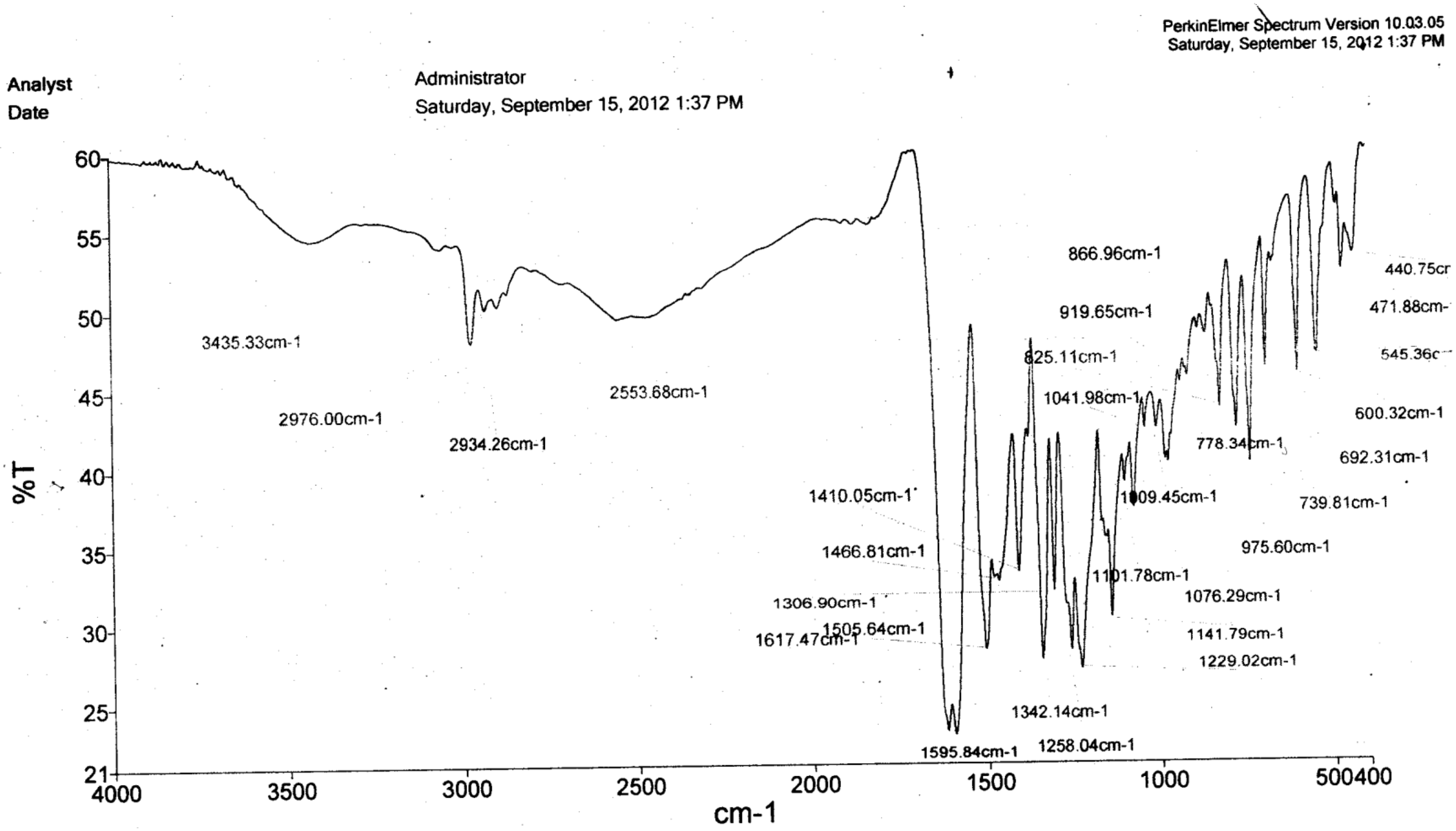

Figure S4: Mass spectrum of **SA1**:

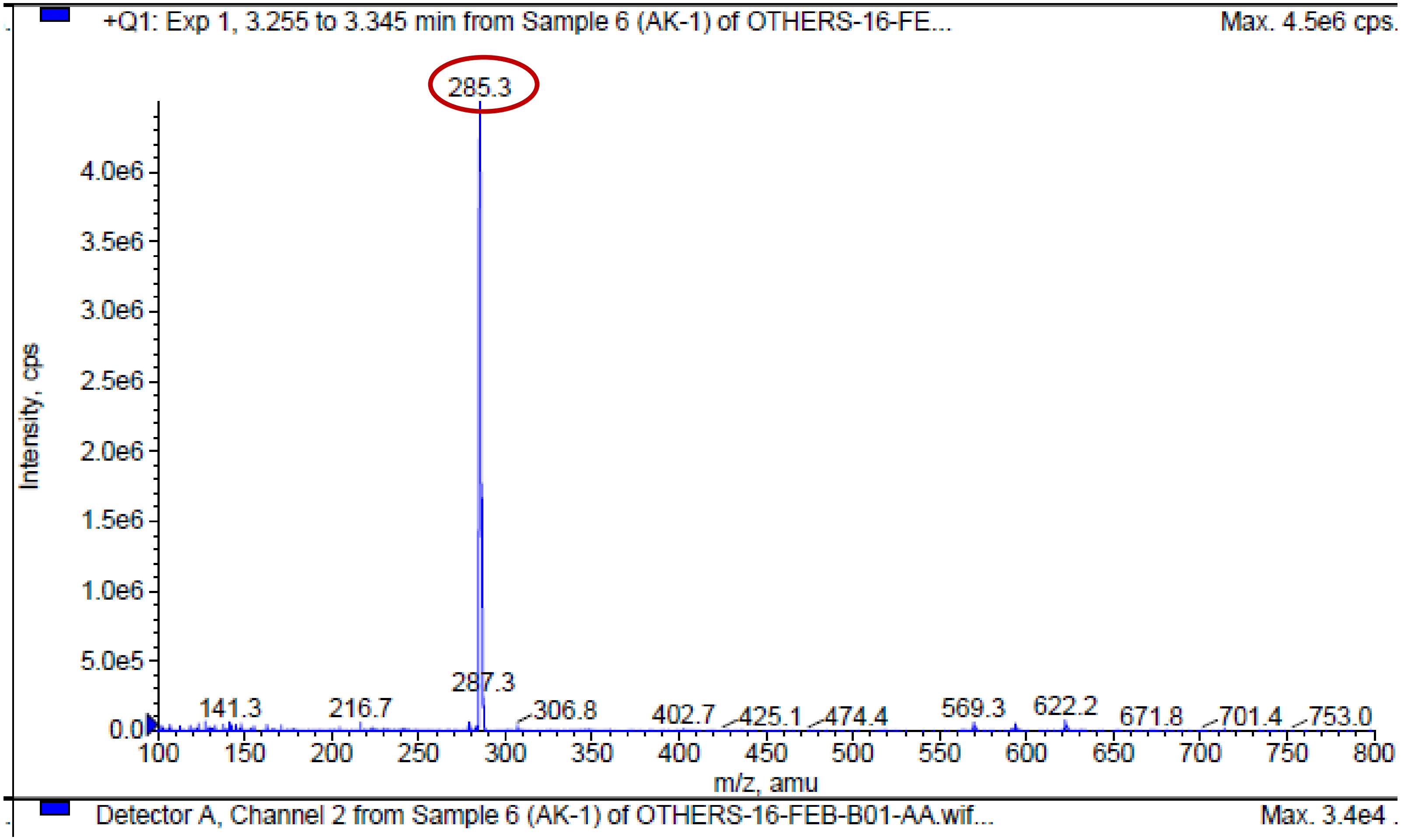

Figure S5: ^{1}H NMR spectrum of **SA1**+Al^{3+} Complex (in DMSO–d$_6$):

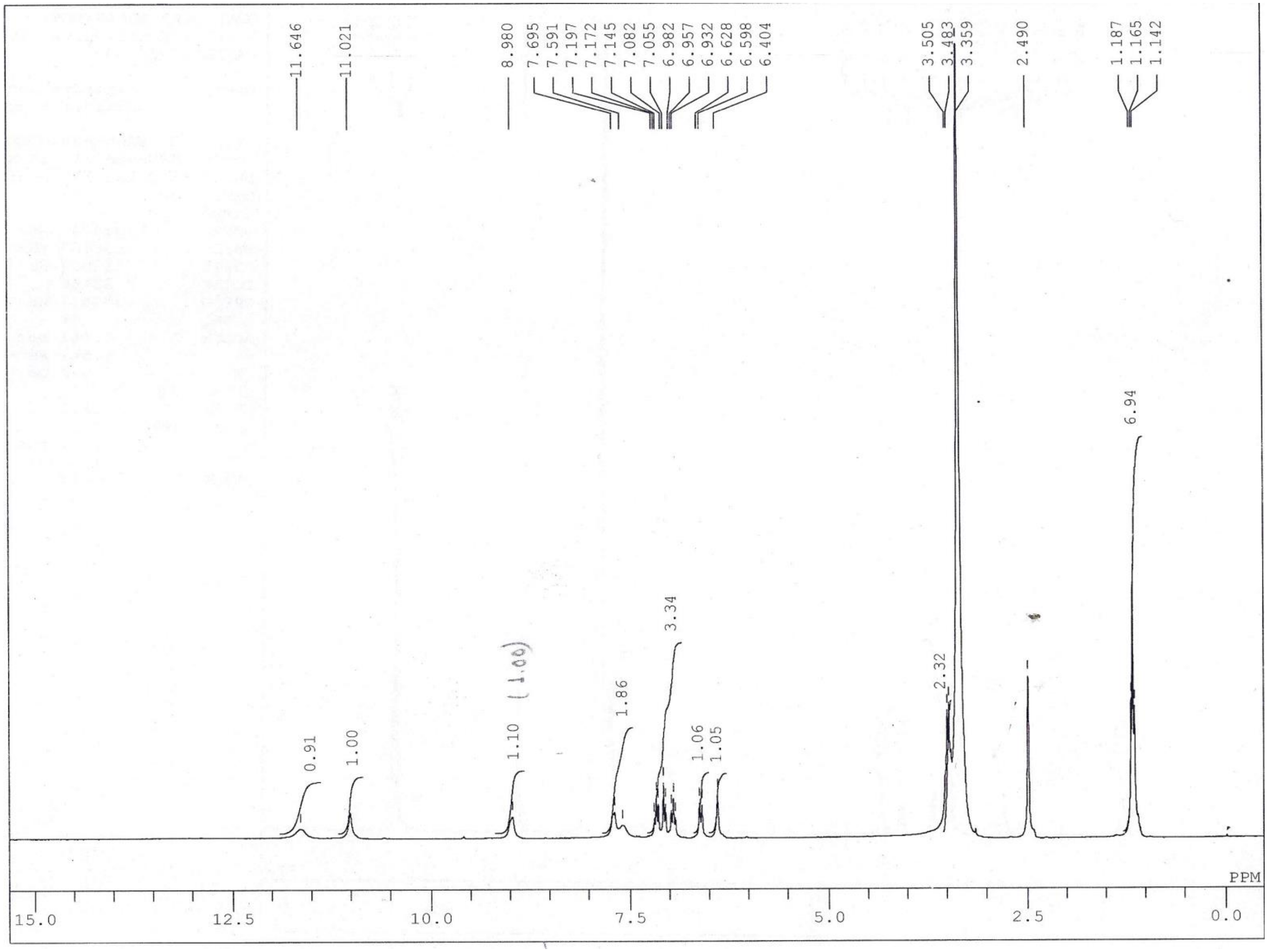

Figure S6: ^{13}C NMR spectrum of **SA1**+Al^{3+} Complex (in DMSO–d$_6$):

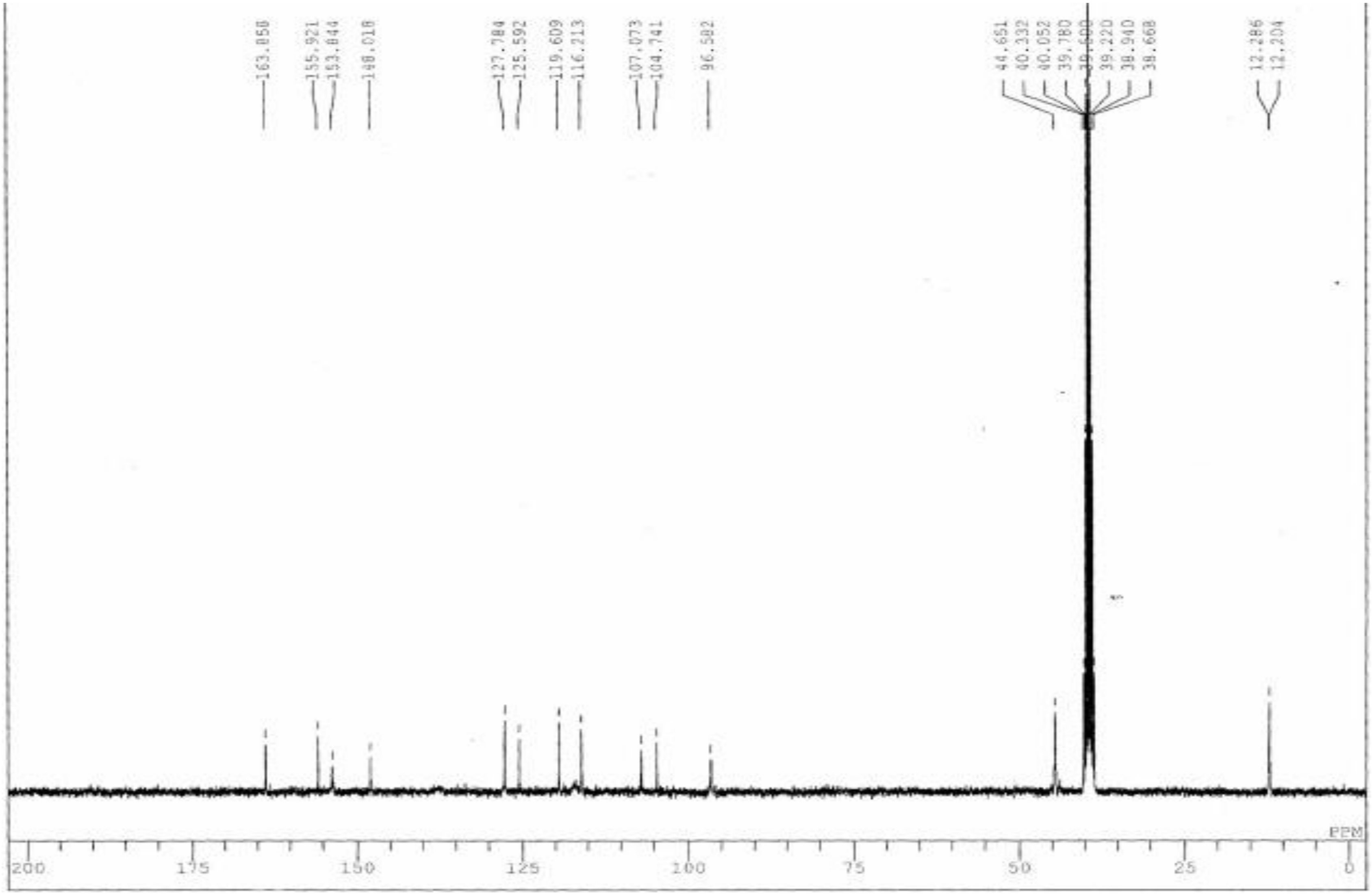

Electronic Supplementary Material (ESI) for Dalton Transactions

Figure S7: IR spectrum of **SA1**+Al^{3+} Complex:

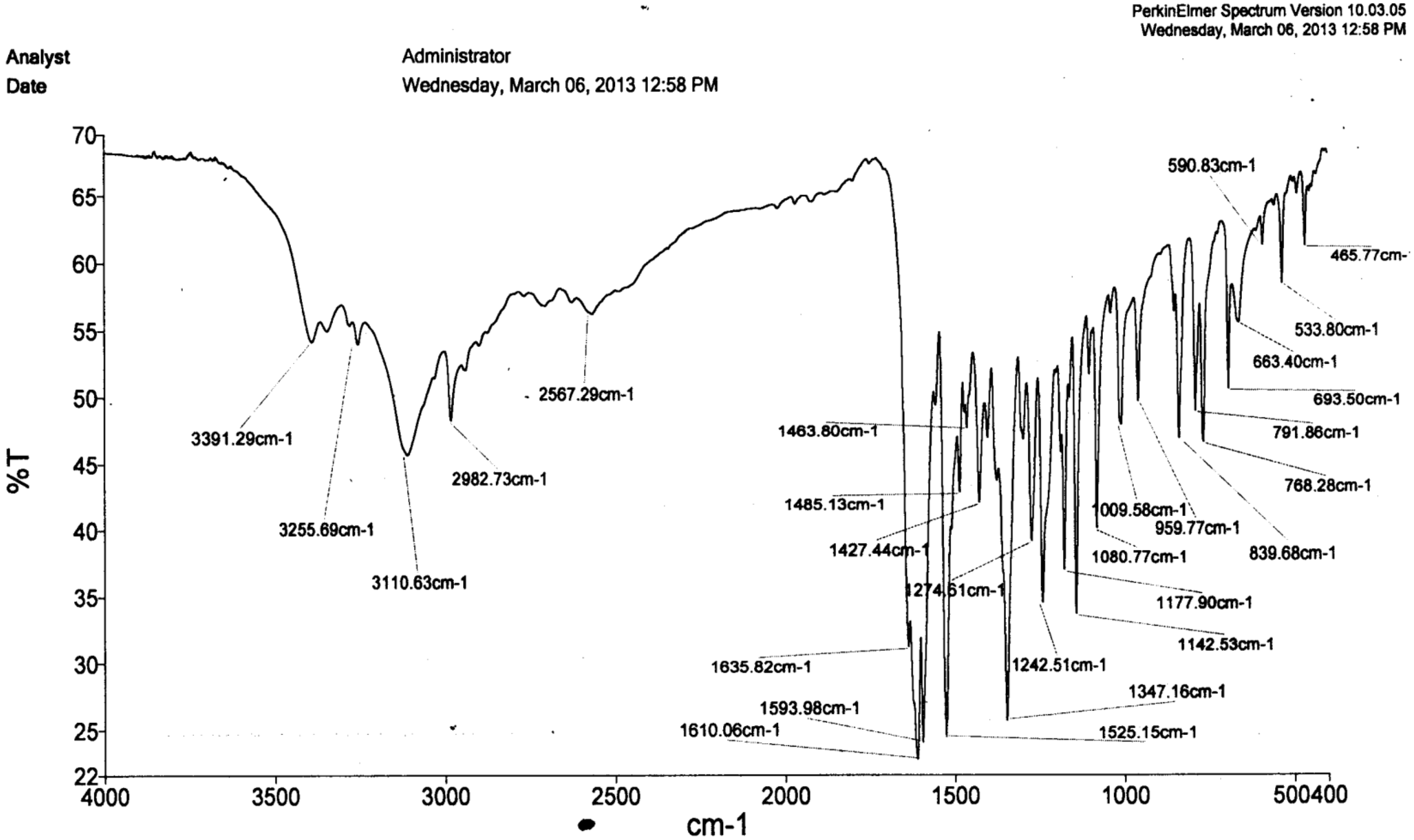

Figure S8: Mass spectrum of **SA1**+Al^{3+} Complex:

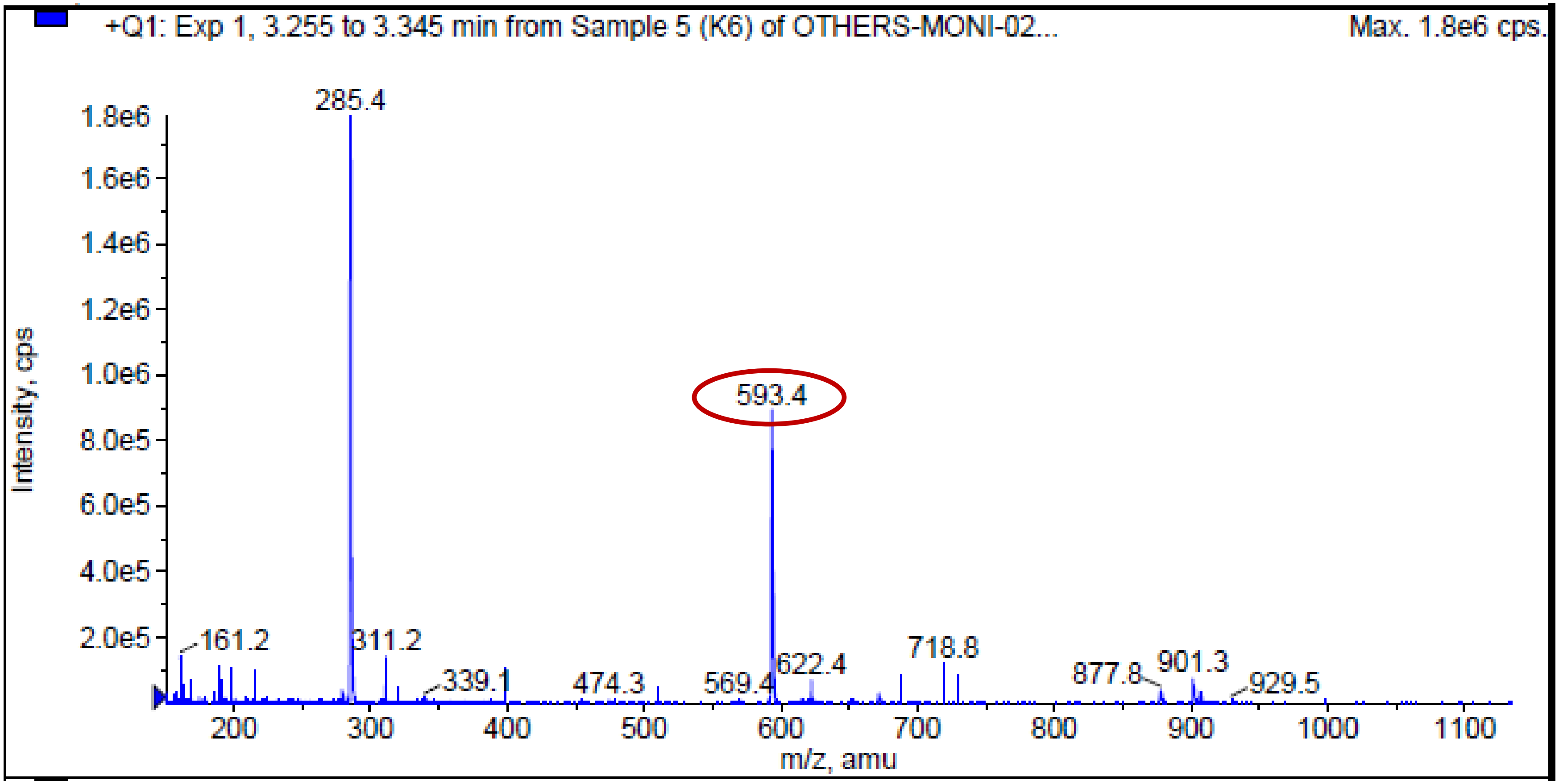

Figure S9: UV–visible spectra of **SA1** with different metal ions at 10 μM in aqueous medium:

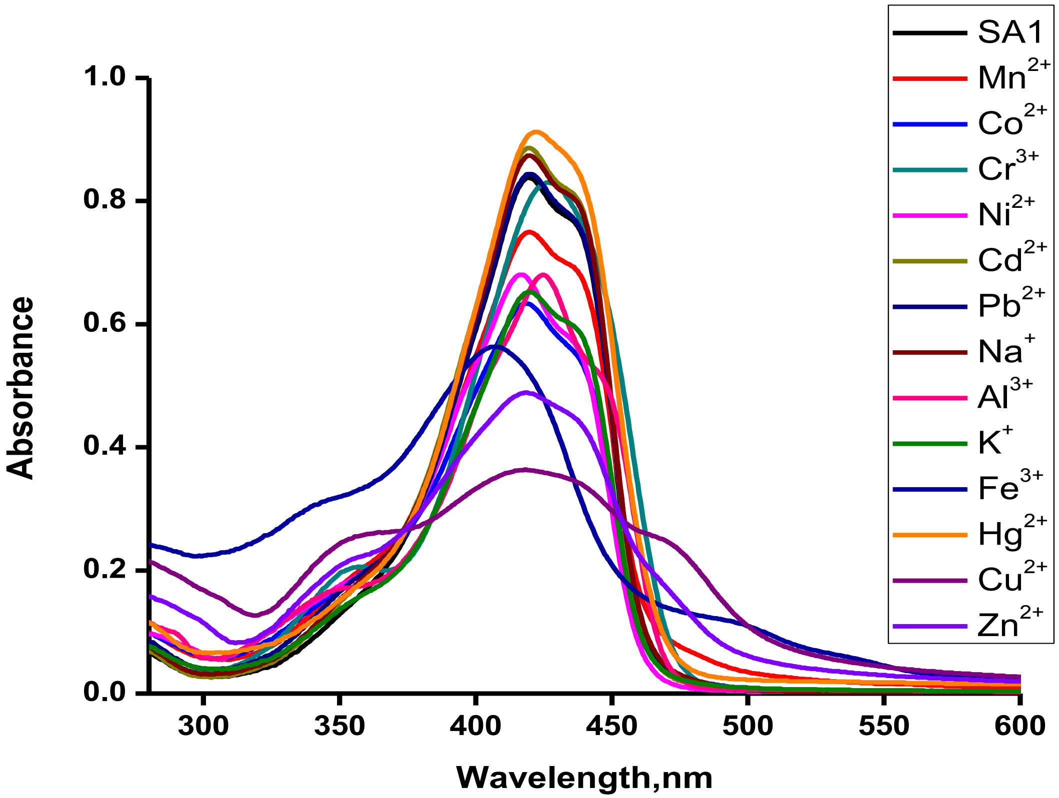

Figure S10: UV-visible titration spectrum of in 10 μM aqueous solution of **SA1** with **(a)** Fe^{3+} and **(b)** Cu^{2+} :

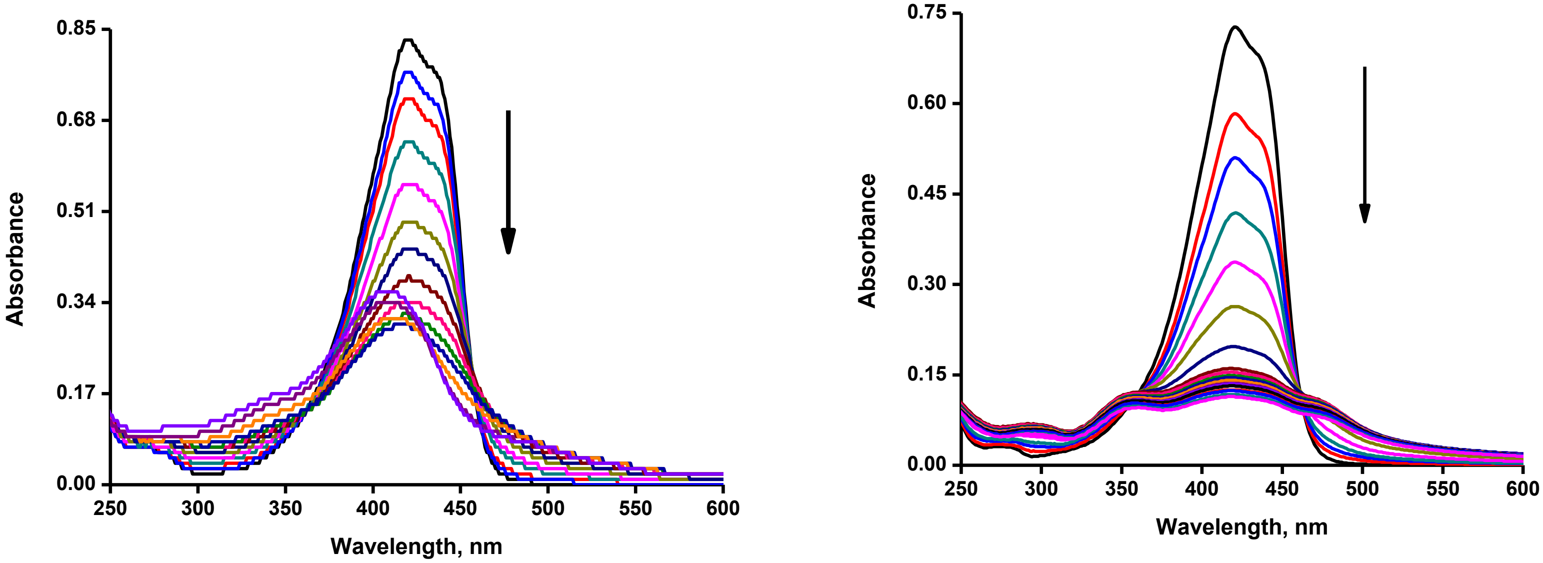

(a) **(b)**

Figure S11: Visible color responses of **SA1** in the presence of various metal ions:

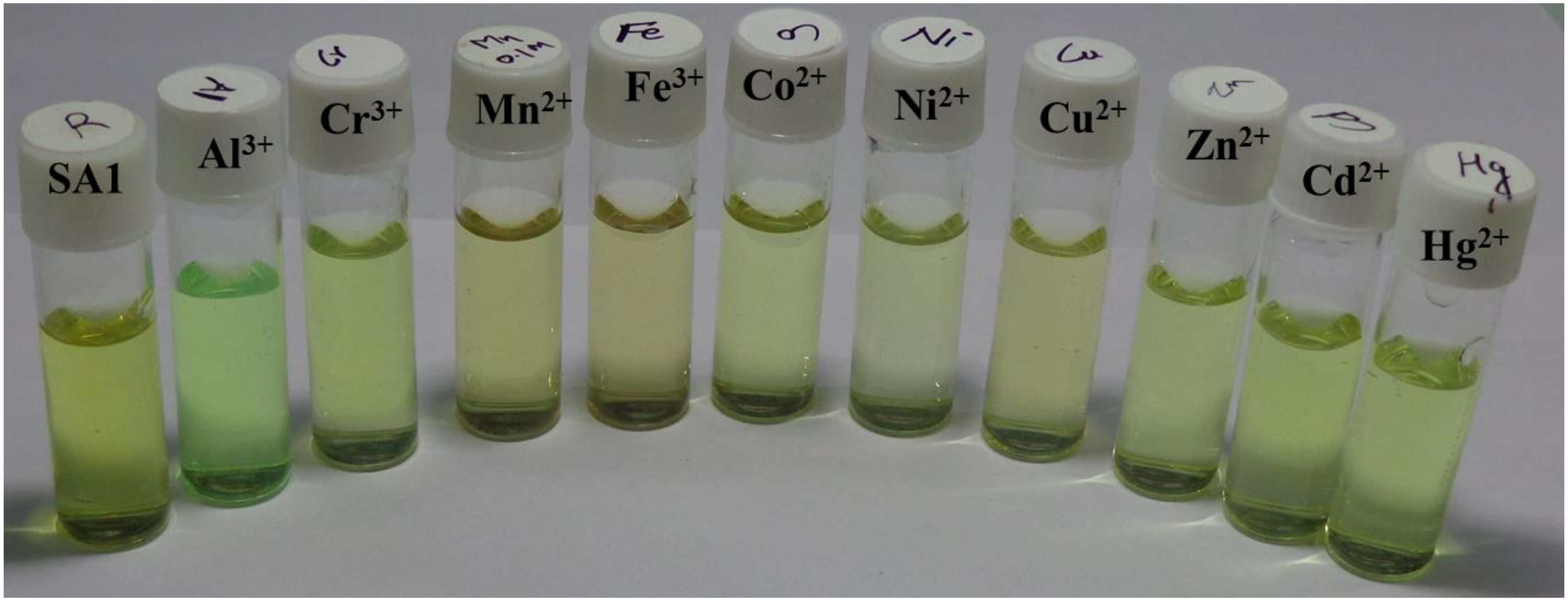

Figure S12: Emission spectra of **SA1** in the presence of $AlCl_3$ and $Al(NO_3)_2$:

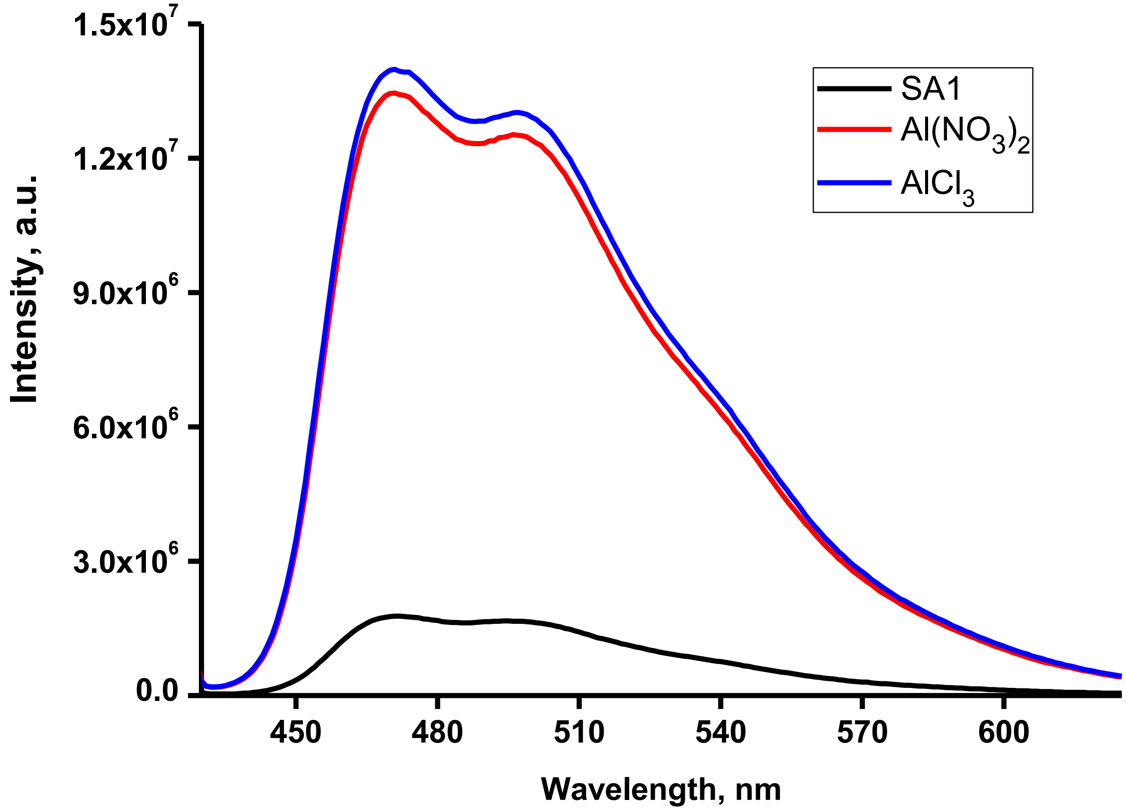

Figure S13: Job's plot of **SA1** with Al^{3+} showing 2:1 binding stoichiometry:

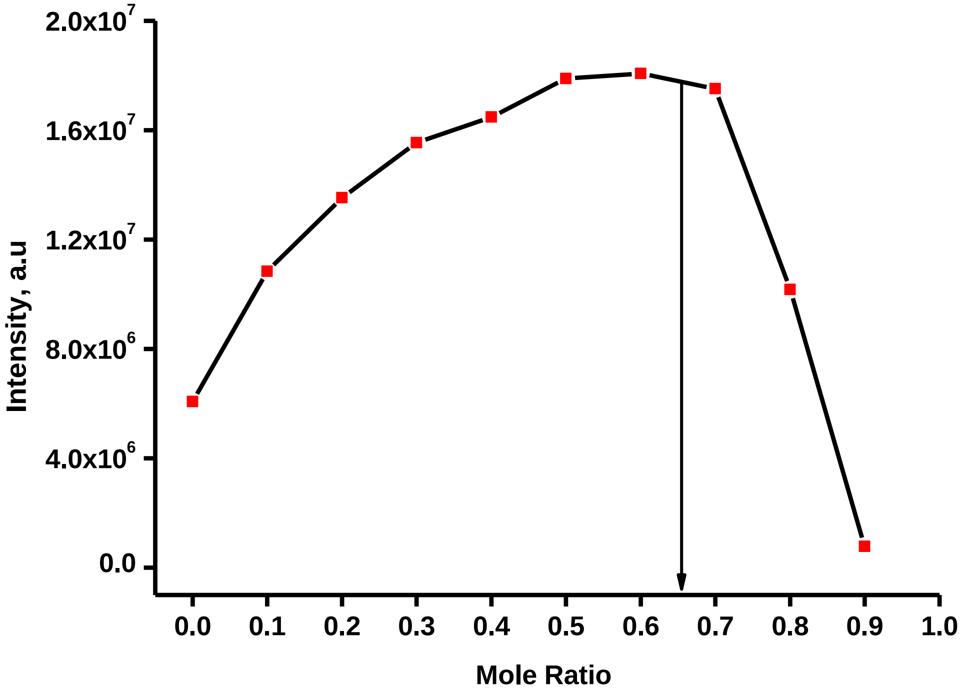

Figure S14: Non-linear fit plot of fluorescence titration data for determination of binding constants:

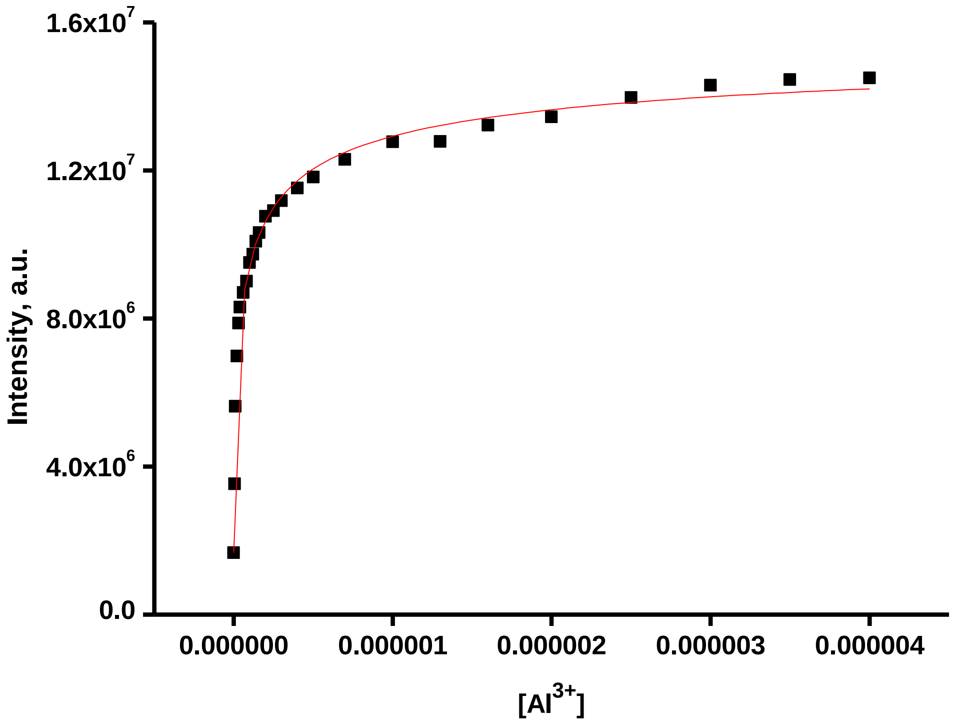

Figure S15: ^{1}H NMR titration studies of **SA1** with Al^{3+}:

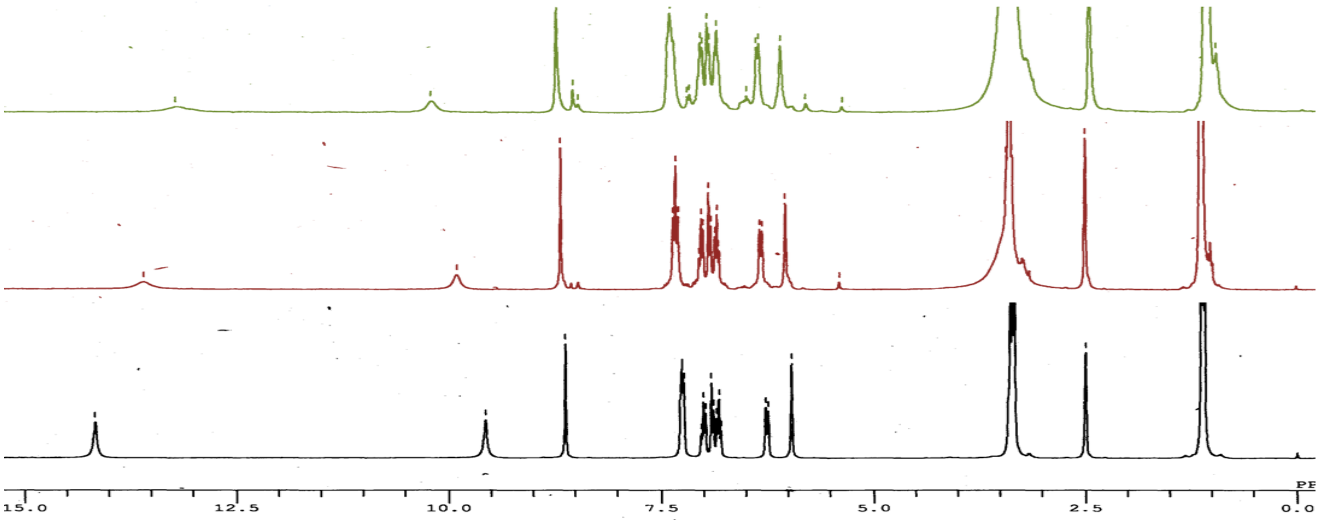

Figure S16: Fluorescence spectral changes of **SA1** and its Al^{3+} complex in the presence of H^+ ion:

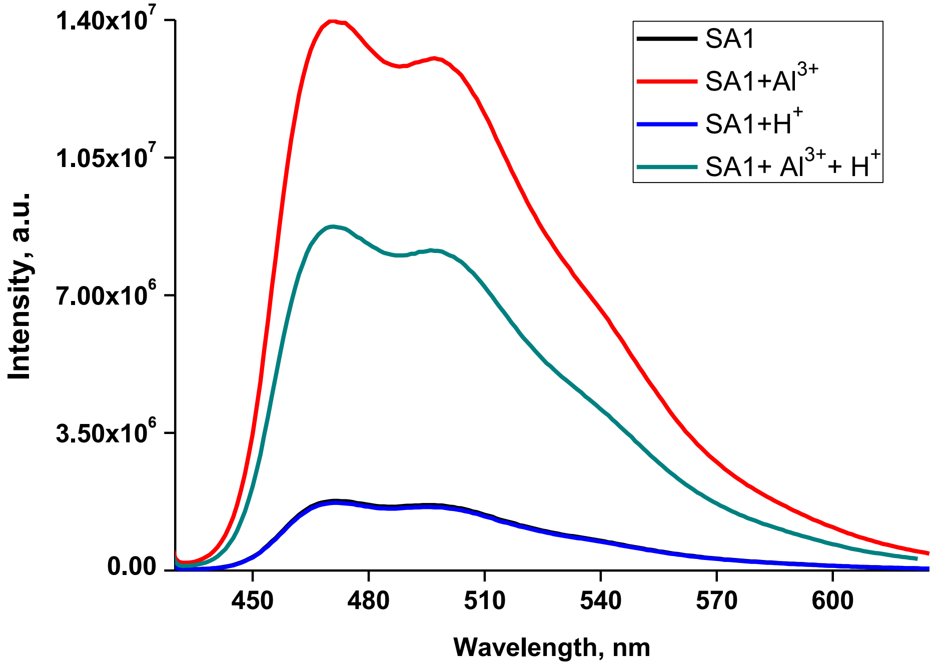

Figure S17: Calibration curve for determination of detection limit of **SA1** for Al^{3+}:

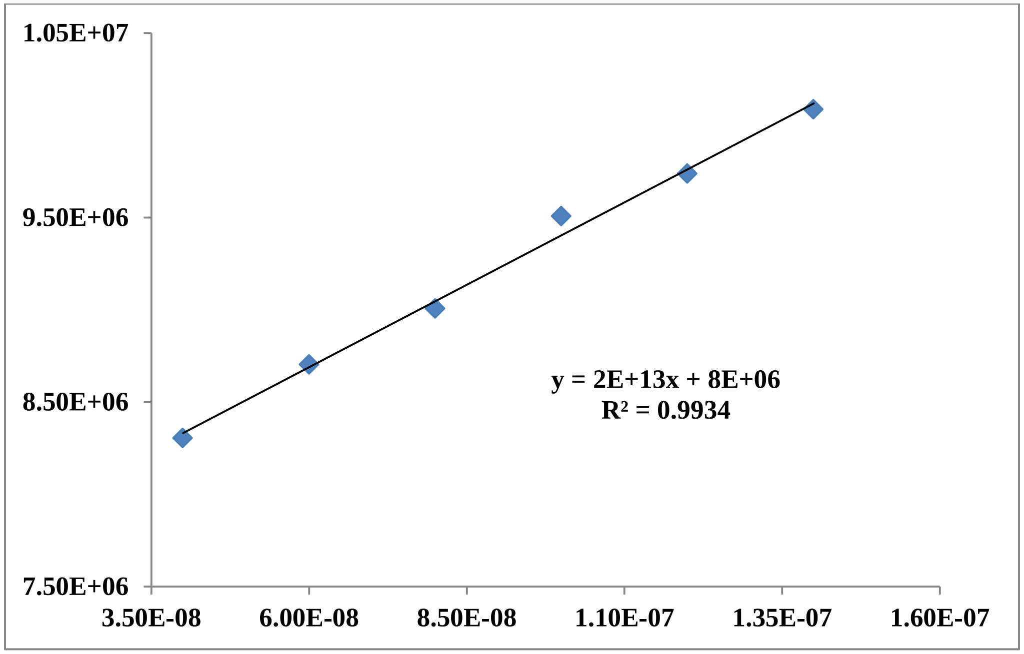

Figure S18: Fluorescence changes at 471 nm of **SA1** (0.5 μM) and **SA1** + Al^{3+} (10 equiv.) in aqueous solution at different pH scale.

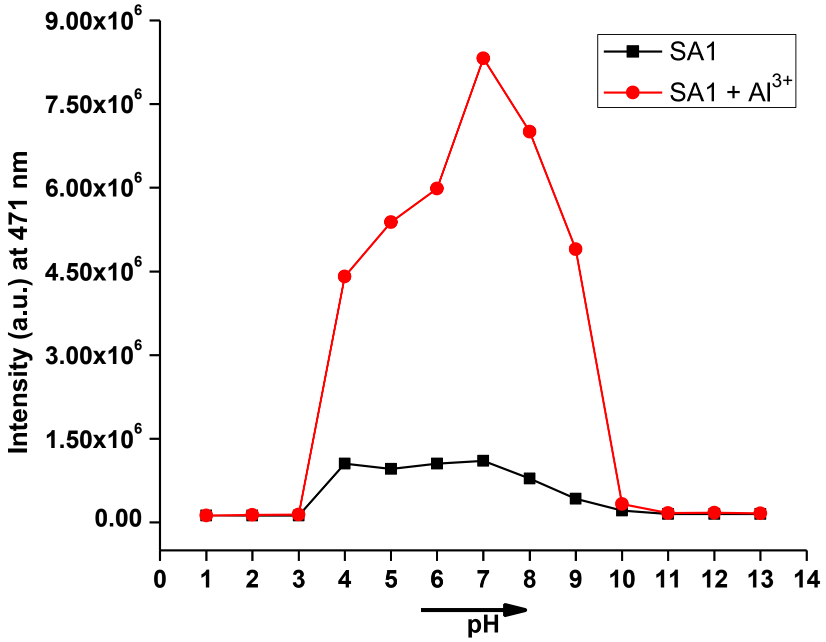

Table 1: Crystal Data and Details of the Structure Determination for **SA1**:

Identification code	**SA1**	**SA1+Cl$^-$**	**SA1+NO$_3^-$**
CCDC No.	**943713**	**959758**	**959759**
Empirical formula	C51 H60 N6 O6	C17 H23 Cl N2 O3	C17 H21 N3 O5
Formula weight	853.05	338.14	347.15
Temperature	293(2) K	293(2) K	293(2) K
Wavelength	0.71073Å	0.71073Å	0.71073Å
Crystal system	Triclinic	Monoclinic,	Monoclinic,
space group	P -1	C 2/c	P 21/c
Unit cell dimensions	a = 11.7339(7)Å alpha = 97.141(4) b = 12.1454(7) Å beta = 105.326(5) c = 17.3108(9)Å gamma = 101.489(5)	a = 18.242(5 Å alpha = 90.000(5) deg. b = 11.925(5) Å beta = 108.114(5) deg. c = 17.097(5) Å gamma = 90.000(5) deg.	a = 8.1825(5) Å alpha = 90 deg. b = 15.0467(11) Å beta = 102.646(7) deg. c = 14.7289(12) Å gamma = 90 deg.
Volume	2290.4(2)Å^3	90.000(5) deg. Å^3	1769.4(2)Å^3
Z	2	8	4
Density (calculated)	1.237 g cm^{-3}	1.273 mg/m^{-3}	1.368 mg/m^{-3}
Absorption coefficient	0.082mm-1	0.232 mm^{-1}	0.097 mm^{-1}
F(000)	912.0	1440	763
Crystal size	0.34 x 0.32 x 0.24 mm	0.42 x 0.38 x 0.32 mm	0.38 x 0.34 x 0.28 mm
Crystal color and habit	yellow and Rectangular	Red and Rectangular	Red and Rectangular
Diffractometer	'Xcalibur, Eos	'Xcalibur, Eos	'Xcalibur, Eos
Theta range for data collection	3.4242 to 29.1795 deg.	2.96 to 29.12 deg.	3.14 to 29.07 deg.
Limiting indices	-8<=h<=11, -11<=k<=10, -16<=l<=16	-22<=h<=18, -16<=k<=11, -21<=l<=21	-10<=h<=10, -17<=k<=18, -18<=l<=8
Reflections collected / unique	9241 / 4266 [R(int) = 0.0203]	8031 / 4002 [R(int) = 0.0580]	7799 / 4010 [R(int) = 0.0278]
Completeness to theta = 25.00	99.3 %	98.8 %	99.7 %
Absorption correction	Semi-empirical from equivalents	Semi-empirical from equivalents	Semi-empirical from equivalents
Refinement method	Full-matrix least-squares on F2	Full-matrix least-squares on F^2	Full-matrix least-squares on F^2
Max. and min. transmission	1.00000 and 0.92705	1.00000 and 0.83830	1.00000 and 0.98287
Data / restraints / parameters	4266 / 0 / 588	4002 / 0 / 215	4010 / 0 / 230
Goodness-of-fit on F^2	1.078	0.979	1.028
Final R indices [I>2sigma(I)]	R1 = 0.0481, wR2 = 0.1197	R1 = 0.0662, wR2 = 0.0832	R1 = 0.0545, wR2 = 0.0978

R indices (all data)	R1 = 0.0640, wR2 = 0.1326	R1 = 0.1826, wR2 = 0.1166	R1 = 0.1180, wR2 = 0.1243
Largest diff. peak and hole	0.329 and -0.270 e. Å $^{-3}$	0.187 and -0.237 e.Å^{-3}	0.191 And -0.193e.Å^{-3}